

**Conference: 40th AIAA/ASME/SAE/ASEE Joint Propulsion Conference and Exhibit
Fort Lauderdale, Florida 11 - 14 Jul 2004**

Authors:

Dr. Francis X. Canning (ISR)
John Cole (MSFC)
Dr. Jonathan Campbell (MSFC)
Edwin Winet (ISR)

Title: The ISR Asymmetrical Capacitor Thruster; Experimental Results and Improved Designs

ABSTRACT

A variety of Asymmetrical Capacitor Thrusters has been built and tested at the Institute for Scientific Research (ISR). The thrust produced for various voltages has been measured, along with the current flowing, both between the plates and to ground through the air (or other gas). VHF radiation due to Trichel pulses has been measured and correlated over short time scales to the current flowing through the capacitor. A series of designs were tested, which were increasingly efficient. Sharp features on the leading capacitor surface (e.g., a disk) were found to increase the thrust. Surprisingly, combining that with sharp wires on the trailing edge of the device produced the largest thrust. Tests were performed for both polarizations of the applied voltage, and for grounding one or the other capacitor plate. In general (but not always) it was found that the direction of the thrust depended on the asymmetry of the capacitor rather than on the polarization of the voltage. While no force was measured in a vacuum, some suggested design changes are given for operation in reduced pressures.

INTRODUCTION

Over Eighty years ago T. T. Brown¹ demonstrated that placing a large voltage across an asymmetrical capacitor produces a force on it. Although many such devices have been built since then, relatively few have been tested systematically. We have built a series of devices and tested them in air, argon and nitrogen, both at atmospheric pressures and down to 2×10^{-5} Torr. Measurements were made of the force produced, current flowing, and VHF radiation emanating from them. In addition, these data were recorded on long time scales up to a resolution of better than a nanosecond. This paper reports on a succession of designs that were built and tested. It describes the motivation for these designs, which produced an increasing amount of thrust, and reports careful test of the resulting designs.

In a separate paper², we have shown that the mechanism for the force is a flow of ions between the plates of the capacitor. That flow occurs primarily in one direction because the device is asymmetrical and charged particles are formed more easily near one of the capacitor electrodes. Electrostatic forces between the capacitor and these ions

collisions with the air. It is useful to keep this model in mind, as it is helpful in designing improved devices and in interpreting the test results.

THE TEST APPARATUS

Mechanical Test Apparatus

A number of Asymmetrical Capacitor Thrusters (ACTs) was tested on one common instrumented test fixture. The test fixture was constructed from Lexan®, with stainless steel for the bearings, and is shown in Figure 1.

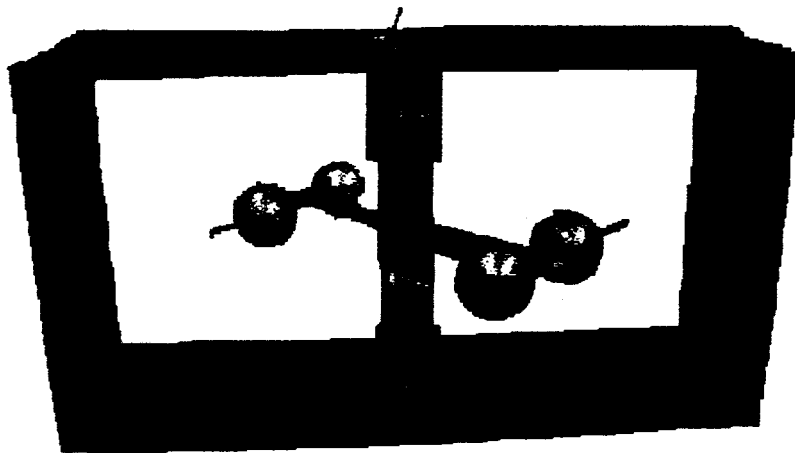


Figure 1. The Test Apparatus.

The approximate size is two feet long, one foot deep and one and a half feet high. This was placed in an aluminum lined wooden box, when tests were performed in our laboratory, and was placed in a steel lined vacuum chamber for tests at reduced pressures.

One of the most difficult design problems was how to put power into the device while it rotated. The device was designed for 50,000 Volts, so standard commutators could not be used since they would cause a breakdown of the air near them. Others have used a needle in a cup as a bearing, which results in a relatively high friction and possibly intermittent electrical conduction. We developed a new design that was low friction, robust to wear, and "anti corona."

It was necessary that the bearings compensate for both axial and radial thrust, while also being an electrical circuit component. This is contrary to standard procedure which avoids passing a current through bearings. Axial thrust is by use of a steel "tooling ball" on the top and bottom of the column, affixed to the aluminum section of the Lexan(r) rotor of either terminal. The tooling ball enters a Teflon(r) lined bushing that serves as both a radial thrust bearing and a holder for a spring loaded brass ball, which is the second half of each axial bearing and the circuit's electrical contact, simultaneously.

Lubrication is augmented for tests at atmospheric pressure by the use of a mixture of graphite and lithium grease where the spheres touch each other. Vacuum chamber applications require diffusion pump oil and graphite mixed, instead, to prevent outgassing. Success of this bearing has been proven by the total elimination of any maintenance and any circuit failure during testing. The design of the lower bearing is shown in Figure 2.

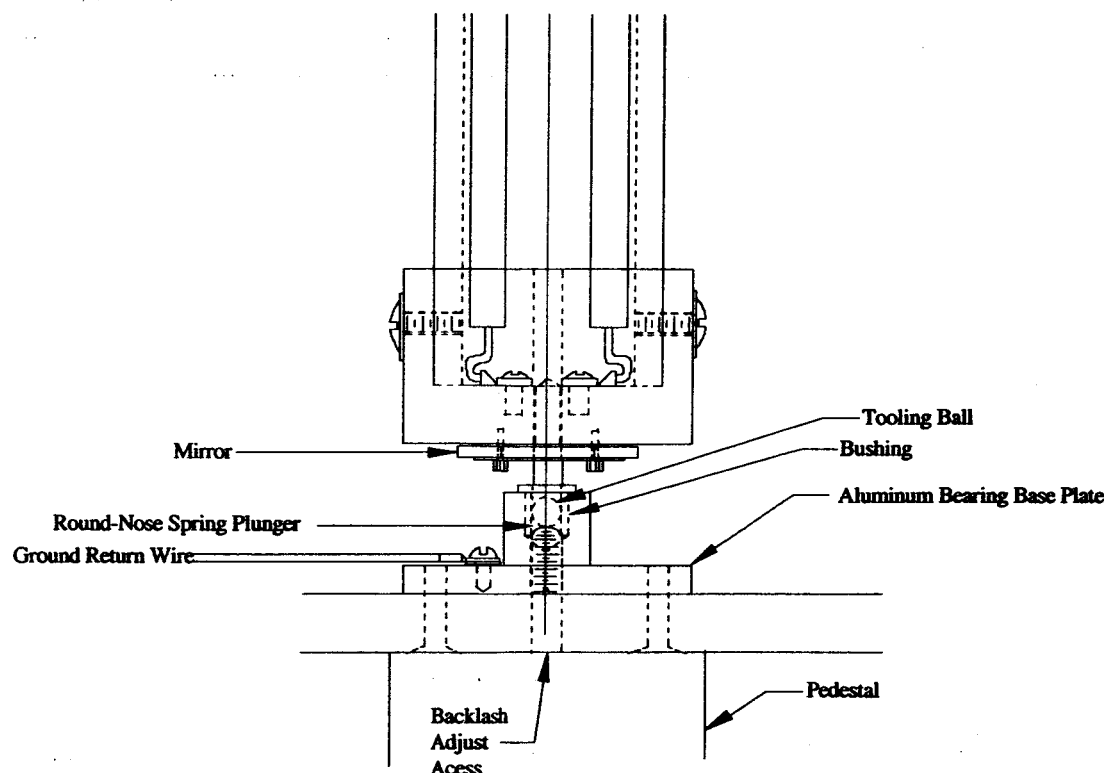


Figure 2. The Lower Bearings.

Considerable effort was made to make the upper bearing corona-proof using standard high voltage terminal techniques. The lower bearing was always kept at ground, so such measures were not necessary for it. Special Teflon corona proof wire, 18 gauge, PTFE, 25 KV rated, was used on all high voltage wiring. Anti-corona techniques were also applied to resistors and other electrical components.

Electrical Test Apparatus

The Asymmetrical Capacitor Thruster was driven by a 50,000 V (maximum) Floating Ground Power Supply. The conducting box surrounding the test device was tied to ground. There is a resistor, R_{LIM} , between the power supply and the ACT which is

designed to limit the current flowing through the circuit for safety purposes, see Figure 3. There was also a spark gap (see Figure 3), which was designed to draw current away when the air broke down. However, this proved ineffective and was removed part way through the testing.

The circuit allows either a positive or a negative ground, due to the polarity reversing connection at the output of the power supply. At the ACT, the polarity could also be reversed, as shown in Figure 3. There were actually two ACTs, one mounted on each arm, as shown in Figure 1. They were wired in parallel, although only one is shown in the schematic. Since two polarities could be reversed, there were four possible circuit combinations. A comparison of the data for all four combinations proved to be very interesting, as will be seen below.

The "Capacitor Operating Voltage" tap, the "Capacitor Current" tap, and the "Ground Return Current" tap, are clearly shown in the schematic of Figure 3. The outputs of these taps are monitored by Fluke Digital Volt Meters (DVMs), a Data Acquisition System (DAS) attached to a personal computer, and an oscilloscope. The oscilloscope provided better time resolution than the DAS. In addition to the measurements shown on the figure, a VHF antenna was used to capture VHF radiation, which was then measured on the DAS and oscilloscope along with the other data.

It should be noted that some of the current reaching the ACT from the power supply will not go to the other plate of the ACT, but rather will go into the air and then find its way to ground by some other route. The amount of current taking this path will be the difference between the "Ground Return Current" and the "Capacitor Current." It would have been preferable to have measured the current passing through the limiting resistor, R_{LIM} , rather than the ground return current. This would have been more difficult, however, due to the high voltage applied. These two currents must have the same time average, although due to capacitance in the power supply they may vary differently over short times. As a result, only the time averaged ground return current (as measured by the DVM) was used.

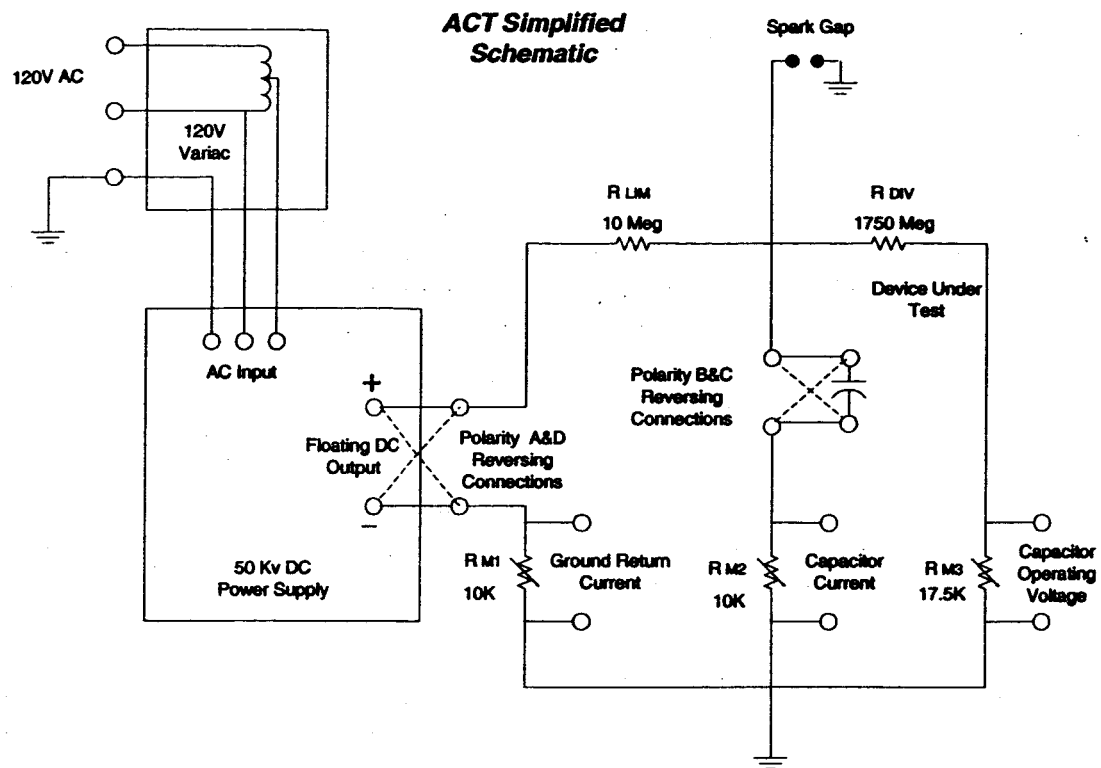


Figure 3. Schematic of Electrical System.

ASYMMETRICAL CAPACITOR THRUSTERS (ACTs) TESTED

A variety of designs of ACTs were tested. For each design, a pair of ACTs was mounted, one at each end of the horizontal arm of the test device, as shown in Figure 1. The design of the first device tested was motivated by the Campbell patent^{3,4}. Since it rotated very slowly, a lighter weight model was produced, as shown in Figure 4. This also rotated slowly, and a series of devices was designed and tested to try to achieve improved performance.

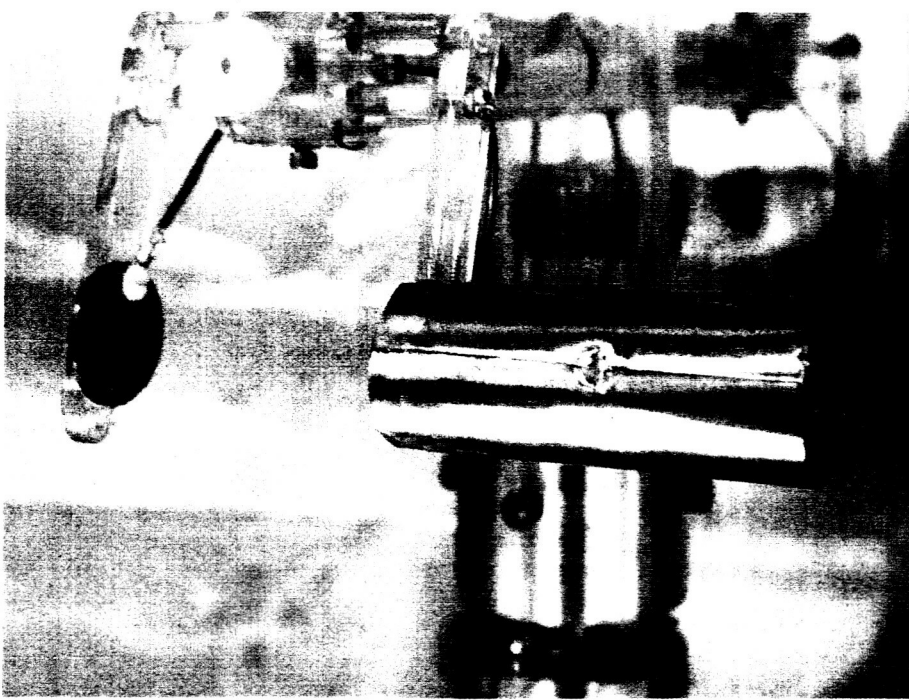


Figure 4. An ACT made from a copper cylinder and disk.

One of the more interesting designs was built from two Styrofoam balls of the same size covered with aluminum foil. This gave a device that was symmetric. Then, wires taken from a screen (such as is used in the window of a house) were added to one of the balls. These wires provide a sharp point that is expected to aid in the formation of ions in the air near the wires. The resulting device is shown in Figure 5.



Figure 5. An ACT constructed from Styrofoam, aluminum foil, and a screen.

The results from this device were very encouraging; it turned significantly faster than the design of Figure 4. This suggested that the principle of operation was related to an asymmetry, where one electrode was "smooth" and the other had a sharp feature. This motivated the design of an ACT that was similar to that of Figure 4, except for this feature, and the ACT of Figure 6 resulted.

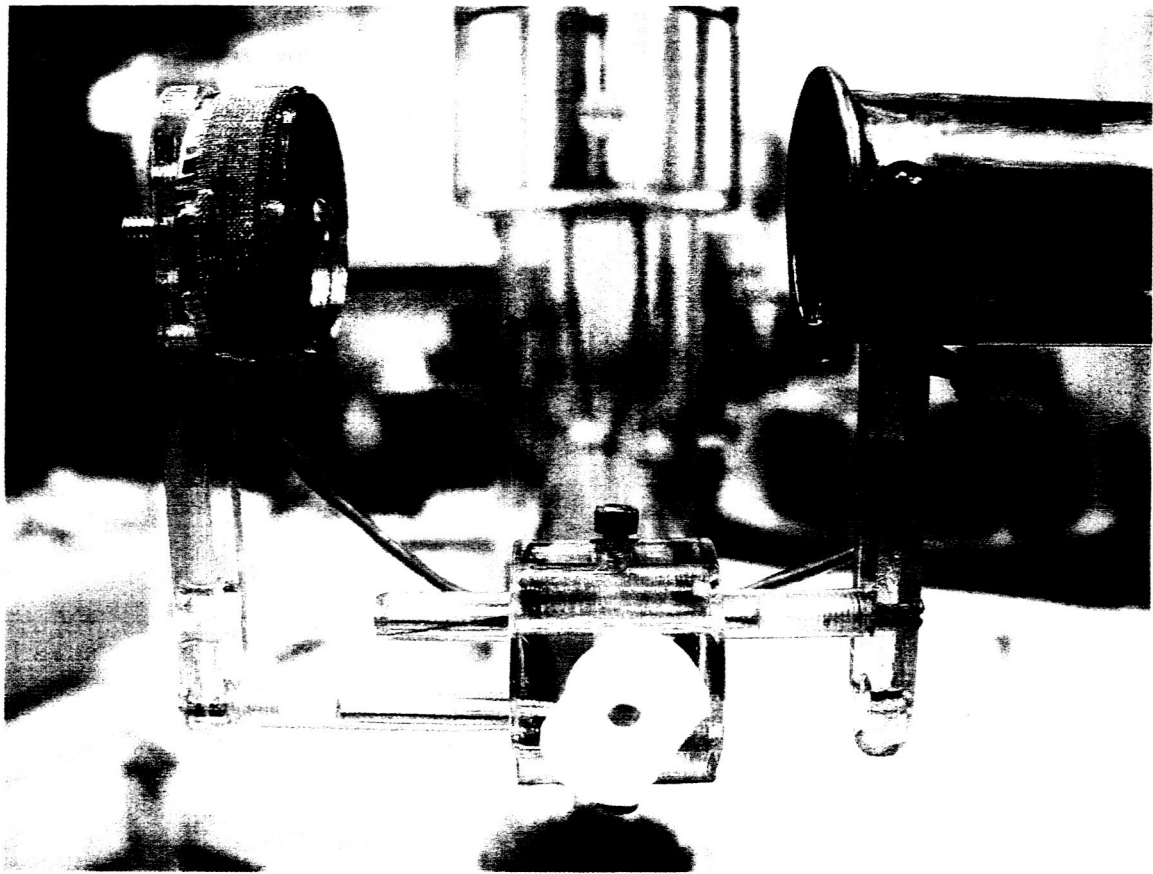


Figure 6. An ACT with sharp features on one electrode, and smoothed features on the other.

The device of Figure 6 produced a much stronger thrust than previous designs. The test device rotated faster than two rotations per second (see the quantitative results below). For completeness, tests were also performed on a device with a dielectric between the electrodes, see Figure 7. This device, which is very similar to that described in Campbell's patents^{3,4}, produced less thrust than a device with points on wires, such as that of Figure 5 as shown by the numerical results reported below.



Figure 7. ACT with dielectric material between the electrode.

Devices Tested in Vacuum Chamber

Tests were performed by mounting a pair of each type of ACT on the test device. Each test placed the test fixture in a rectangular box with conducting sides which were grounded. Early tests in our laboratory produced several devices which barely moved, if at all. A series of devices were constructed with improved performance. For example, the two balls with a screen (see Figure 5) achieved sixty RPM.

For the tests to be performed in a vacuum chamber, four devices were selected. These devices are as described in Table 1.

TABLE 1

Device #	Shown in Figure #	Description
1	4	A disk and a cylinder made of copper
2	7	A disk and a cylinder, with dielectric between
3	6	A disk and a cylinder, with a screen on the disk and a rounded collar on the cylinder
4	6*	A disk and a cylinder, with a screen on the disk and a rounded collar on the cylinder and with a screen (and wire ends) on the end of the cylinder farthest from the disk

*Note: Device 4 differs from Device 3 in whether there is a screen on the end of the cylinder that is not shown in Figure 6.

In addition to having four devices to test, there were four circuits that were used to test these devices. The circuits differed according to which electrode was positive and according to which electrode was grounded. These choices were effected by reversing the polarity in the two locations shown on Figure 3. For clarity, these four circuits are described as Circuits A, B, C, and D, as shown in Figure 8.

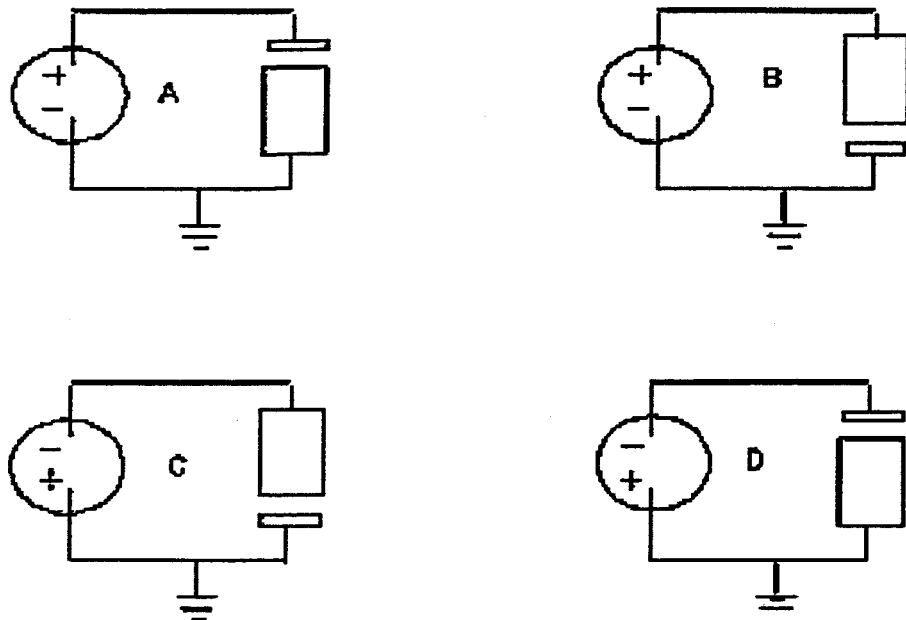


Figure 8. The four circuits, which vary according to which electrode is positive and which electrode is grounded.

MEASUREMENT OF THE TORQUE GENERATED

Each pair of ACTs was tested by applying a voltage, waiting for the rotation rate to increase to its maximum, and recording that maximum rotation rate. It was then necessary to compute the force that was required to achieve that rotation rate. This may be done by assuming that the driving torque is equal to the frictional torque from all sources, when the rotation rate is constant. This frictional torque may be computed from a measurement of the moment of inertia of the rotating element and a measurement of its deceleration when the driving force is removed.

The moments of inertia were computed from measurements of the period of rotation. The test fixture was disassembled, and rotating element was suspended from a torsion fiber. This fiber was a steel guitar string with a diameter of 0.30 millimeters. The results are shown in Table 2. The effective radius shown there is for a hypothetical device, with all of its mass at the same radius. The period and mass were measured directly. The Moment of Inertia and effective radius are computed quantities.

The stiffness of the torsion pendulum was determined by suspending two cylindrically shaped masses and measuring their periods. The first has a radius of 3.79 cm and a mass of 500 grams. The second had a radius of 4.74 cm and a mass of 1,000 grams. Thus moments of inertia of these masses were computed from $\frac{1}{2} m r^2$ as 3,591 and 11,234 gm \cdot cm 2 respectively. The square root of the ratios of the moments of inertia is 1.769. The periods of these two cylindrical masses were 6.25 and 11.13 seconds. The ratios of these periods is 1.781, which agrees with the 1.769 computed above within a percent.

TABLE 2

Device	Moment of Inertia (gm-cm **^2)	Mass (gm)	Radius (Effective) (cm)	Period (seconds)
1	54,660	936	7.64	49.165
2	43,430	914	6.89	43.822
3	62,733	964	8.07	52.671
4	76,660	1,000	8.76	58.227

The periods were measured by timing ten periods and dividing by ten. This was done multiple times, and the results were consistent to better than a tenth of a second for the period. This agrees with the consistency check above which also suggests that the times measured are accurate to better than one percent. Since the moment of inertia is proportional to the square of the period, this suggests that the moments of inertia found were accurate within two percent, barring other systematic errors.

One additional consistency check was performed. All of the measurements that were used in the computation were performed letting the torsion pendulum oscillate through 180 degrees plus and minus rotation. As a test, measurements were also performed using a 90 degree plus and minus rotation. The period measured was slightly shorter, but still within one percent of the other value measured. Thus, the difference found was within our ability to measure the period. For all these reasons, we believe that the moments of inertia given above are accurate to approximately two percent. This will be much more accurate than our ability to measure decelerations.

Deceleration as a Function of Velocity:

Deceleration was measured for the assembled test fixture, rotating on its bearings. The raw data that were recorded was the time at which each successive rotation of one sixth of a revolution occurred. The data acquisition system passed the raw data to LabView software which then computed an approximate (smoothed) velocity as a function of time. An algorithm was used to detect missing data (when one of the impulses for a specific sixth-turn is missed) and to still provide an accurate velocity.

The acceleration is the time derivative of the velocity. The first attempts at taking differences of successive velocities and dividing by the time difference provided poor results. In hindsight this was to be expected since this is effectively the second derivative of data with noise present. The solution was to provide some smoothing in computing the derivative of the velocity. This was accomplished by using a method which is closely related to linear regression. That method is to perform a least squares fit of a straight line to each five successive velocities. At time step j , the acceleration, a_j , was computed as:

$$a_j = \frac{5 \sum_{k=j-2}^{j+2} t_k v_k - \sum_{k=j-2}^{j+2} t_k \sum_{k=j-2}^{j+2} v_k}{5 \sum_{k=j-2}^{j+2} t_k^2 - \left(\sum_{k=j-2}^{j+2} t_k \right)^2}$$

This formula gives the acceleration as the slope of the resulting line. Minus this acceleration, or the deceleration, is plotted on the figures that follow. These were found to be significantly smoother than the data that were not smoothed (although significant jitter is still evident).

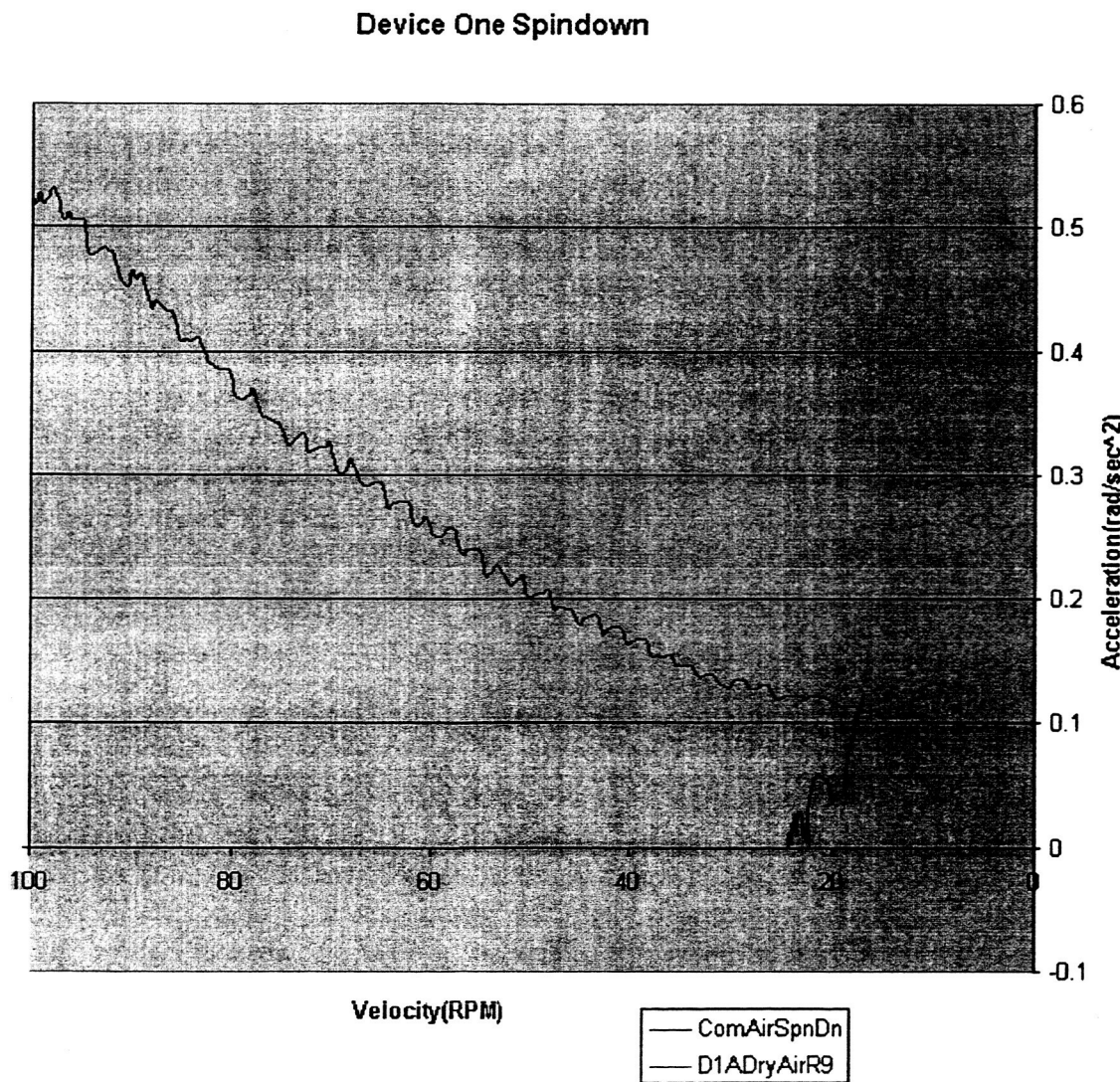


Figure 9. The deceleration of Device 1 as a function of velocity.

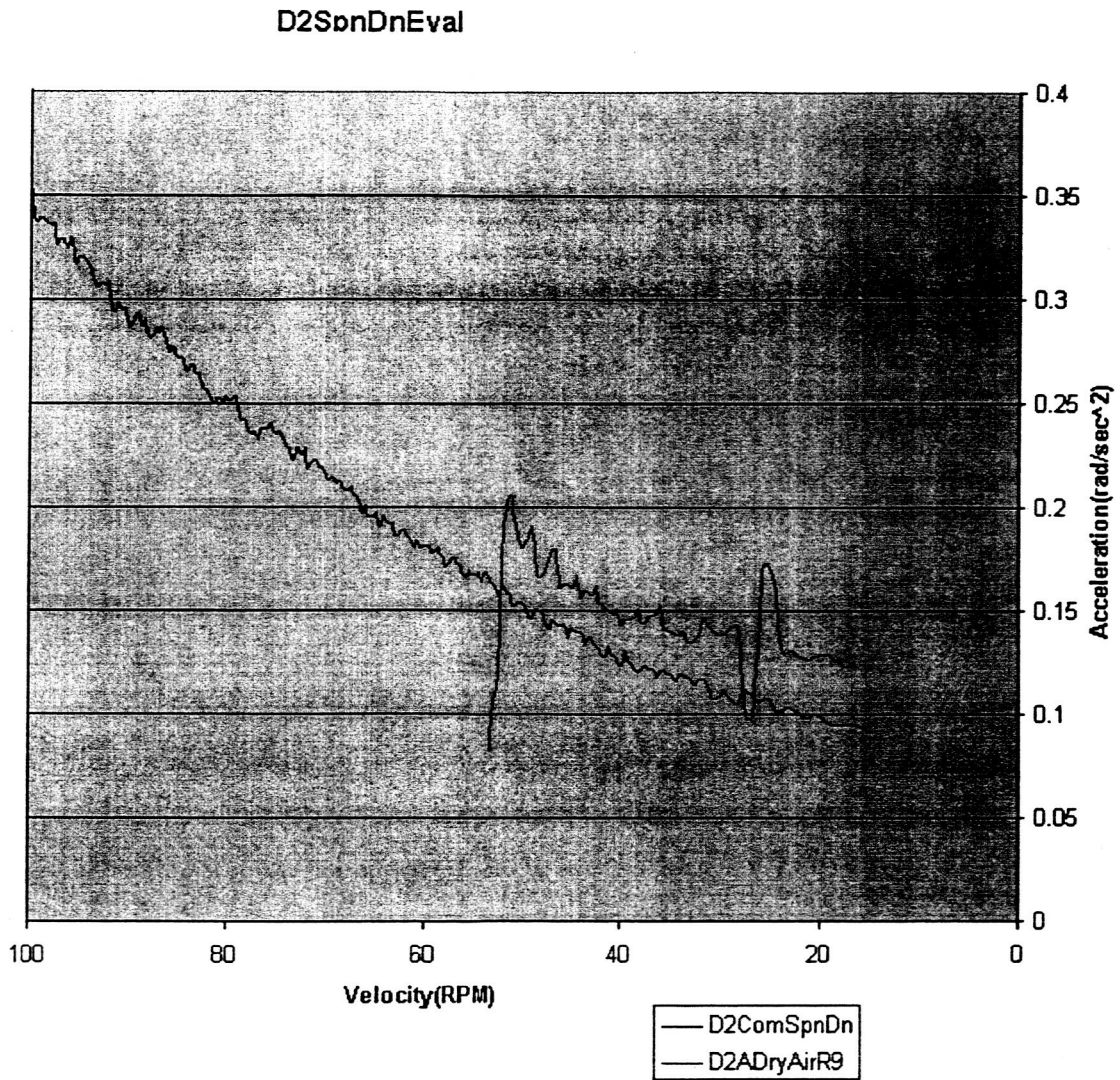


Figure 10. The deceleration of Device 2 as a function of velocity.

Figures 9 through 12 show the deceleration as a function of time for each ACT mounted on the test fixture. The different curves on each figure correspond to different ways in which the initial rotation rate was achieved and also different pressures and gasses. Some of the curves result from achieving an initial rotation rate by running the ACT using a constant applied voltage. There was some concern that there might be a residual charge or similar effect which would confound the results. For this reason, each figure also shows a curve for a run where the rotation rate was achieved using compressed air to initiate the rotation. These tests were all done in our laboratory using room air at atmospheric pressure. The corresponding curves on the figures are labeled with "CommAir" or "Comm." It can be seen that there is no clear systematic effect distinguishing the runs which used compressed air from other runs.

D3DSpnDnEval

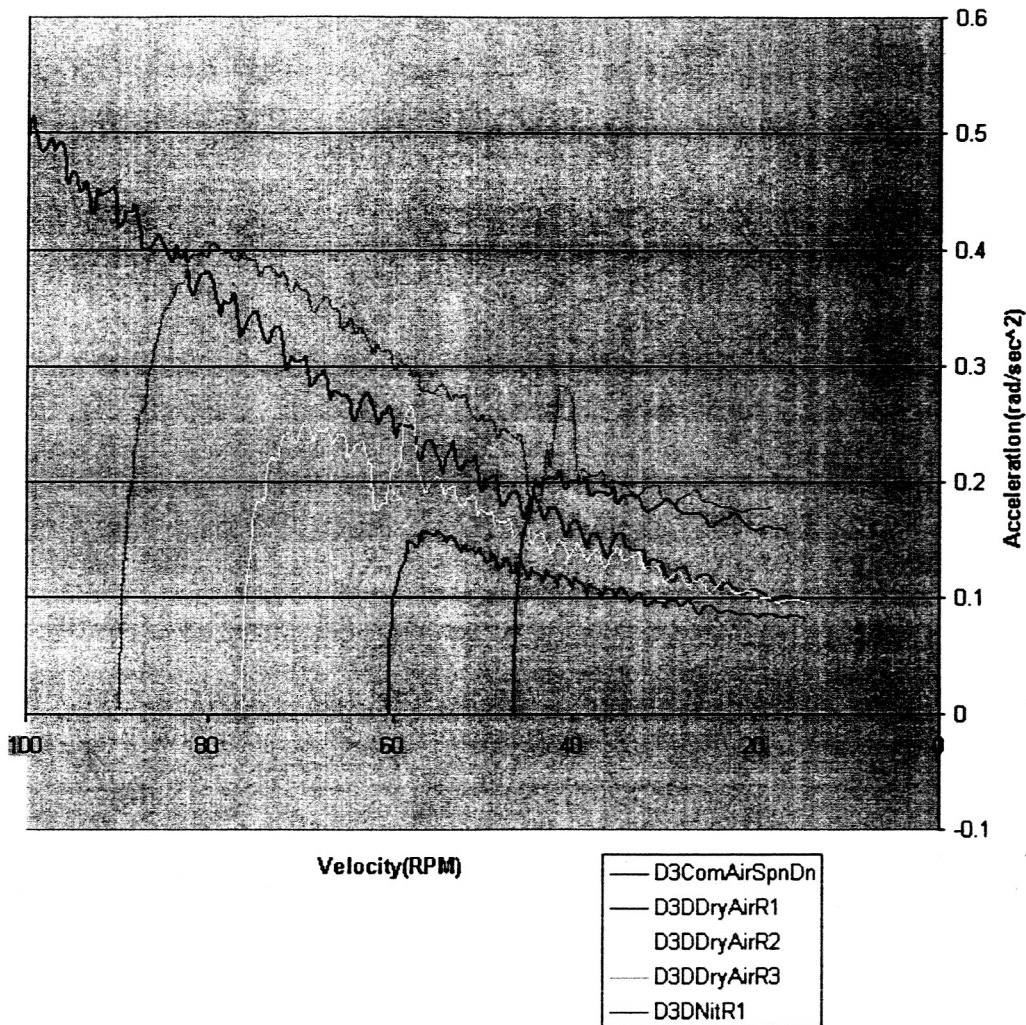


Figure 11. The deceleration of Device 3 as a function of velocity.

On Figures 9 and 10, the runs labeled D1AdryAirR9 and D2AdryAirR9 are both for runs in dry (moisture removed) air at 700 Torr. They are for Devices 1 and 2 respectively and both used Circuit A. On Figure 11, all of the runs are for Device 3 using circuit D. The runs in air labeled R1, R2, and R3 are at a pressure of 300, 500, and 700 Torr respectively. The run in nitrogen was performed at 700 Torr. It is not clear why run D3DdryAirR3 would have the weakest deceleration, since air resistance might be expected to be stronger than for R1 and R2. One might speculate that residual charge in the vacuum chamber might make these results more variable. This speculation might also suggest that Device 4 may have less variability, since the wires on the trailing edge of the cylinder may remove ions from the air.

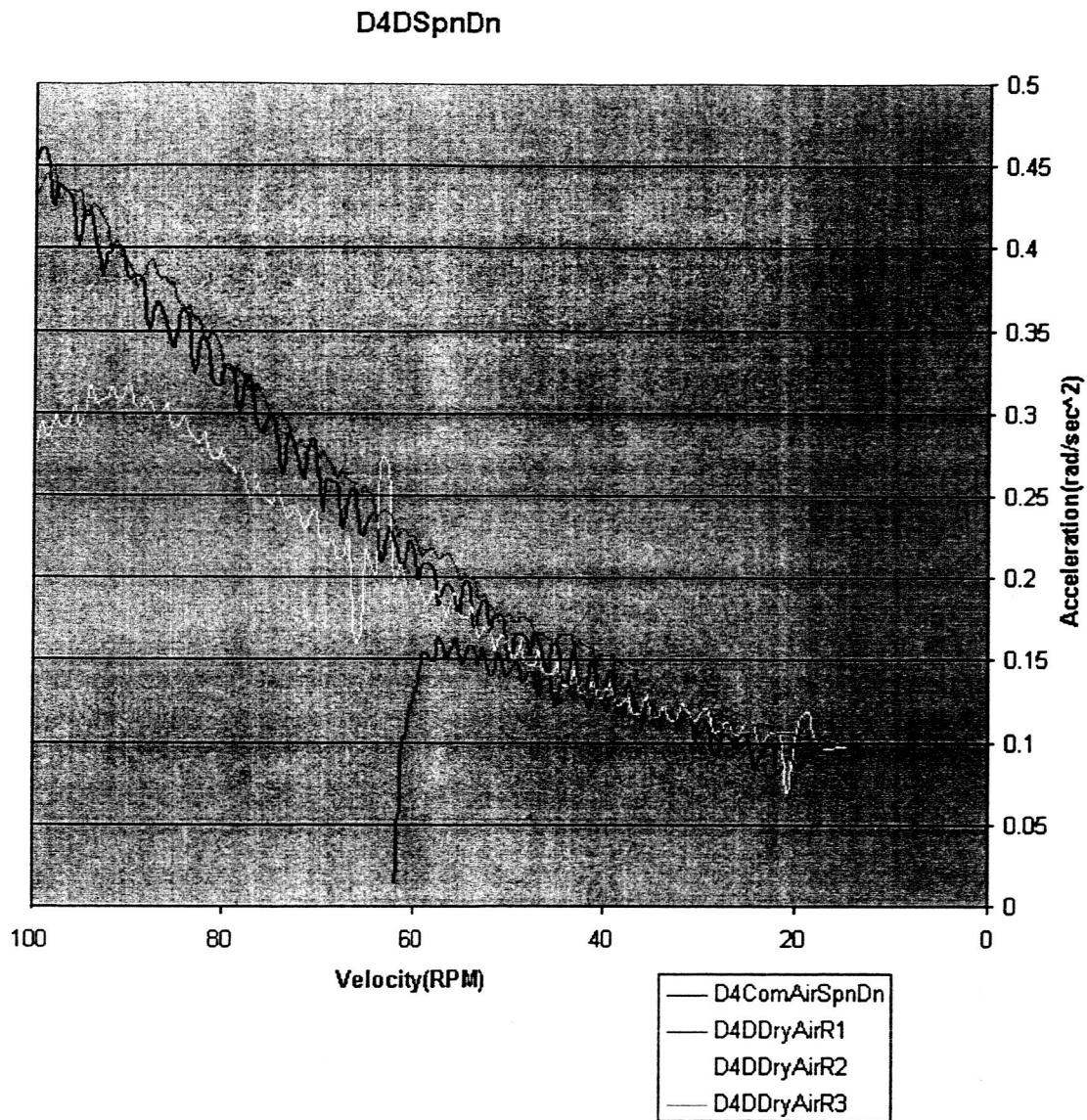


Figure 12. The deceleration of Device 4 as a function of velocity.

Figure 12 shows runs for Device 4 using circuit D. The runs R1, R2, and R3 are at pressures of 300, 500, and 700 Torr respectively. Here, all of the curves show nearly the same deceleration as a function of velocity. For later calculations, for each device we will use the curve for the compressed air as a reasonable representation of the average result.

MEASUREMENTS OF ACT OPERATION

Data were acquired over several time scales. Steady state data were acquired by digital volt meters, a data acquisition system for scales of minutes down to milliseconds, and a high speed oscilloscope for data resolved to better than a nanosecond. When the ACTs were run in air, the current often flowed in bursts, called Trichel pulses. This was the only physical effect that changed fast enough to require the fast resolution of the oscilloscope.



Figure 13. The top trace shows the current flowing out of the ACT and the bottom trace gives the radiation received from a VHF antenna. The horizontal scale is four milliseconds per box. The data was acquired for operation in room air.

Figure 13 shows that the received pulses of radiation coincide with the bursts of current that flow. (The antenna's response has broadened these pulses in time.) Trichel pulses are an avalanche phenomena, which have a current that rises exponentially, and then saturates. Data taken on a nanosecond time scale confirmed that behavior. We also observed that when ACTs operated in argon and nitrogen there were no Trichel pulses although a thrust was still produced. Thus, we do not believe that Trichel pulses are intrinsically involved in creating the force.

There has been speculation about whether ACTs can operate in a vacuum, even though this does not appear possible based on generally accepted physical mechanisms that have been identified. To provide one test of this possibility, we considered the data from the best performing devices, Devices 3 and 4. Figure 14 shows data from their tests in the vacuum chamber using dry air.

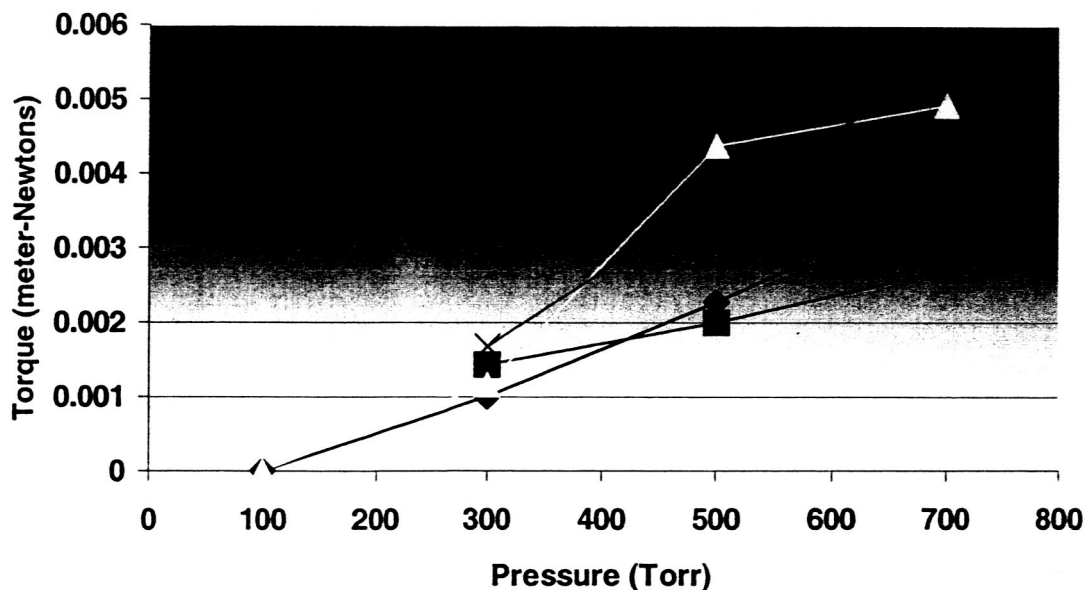


Figure 14. Speed achieved for various devices and circuits, in dry air in a vacuum chamber. The results for Device 3 are plotted using diamonds for Circuit A and squares for Circuit D. The results for Device 4 are plotted using triangles for Circuit A and using the shape "x" for Circuit D. The data points are joined with lines as a guide for the eye (no prediction is implied).

The different plots on Figure 14 generally do not lie along straight lines. In particular, the plot for Device 4 Circuit A is concave down and for Device 3 Circuit D is slightly concave up. Not much of importance should be read into this, however. For example, if a specific device were designed to have an optimized performance at 300 Torr, that alone might cause this slight concave up behavior. On the other hand, if a device were designed with the optimum gap size for operation at atmospheric pressure, then the curve might be strongly concave down.

From these plots, we see no evidence that an ACT would work at zero pressure. All of the plots shown are headed towards approximately zero torque by the time the pressure reaches zero. However, we do expect that if we were asked to design a device to work at a pressure such as 300 Torr, then we could improve on the results shown here. This could be accomplished using simple design rules, such as finding the smallest gap necessary to prevent breakdown for the design voltage.

Through the course of this testing, a few patterns became very apparent. The most obvious pattern found was that Device 4 was the best performing design with respect to both total thrust produced and thrust produced for power input. However, Device 4 turned best with a negative charge on the small electrode (D), while all other devices turned better with a positive small electrode (A). Also, all of the devices produced the most thrust when the trailing electrode was grounded. Table 1 gives information for each run where rotation occurred while in a dry air environment in the vacuum chamber. The comparative performance of each device improved as the device number increased.

Table 3 Device Performance in Dry Air

Device		Configuration A			Configuration D		
1	Pressure (mm Hg)	700					
	Capacitor Voltage (kV)	40					
	Capacitor Current (μ A)	250					
	Ground Current (μ A)	250					
	Rotation Speed (RPM)	24					
2	Pressure (mm Hg)	700					
	Voltage (kV)	35					
	Capacitor Current (μ A)	168					
	Ground Current (μ A)	180					
	Rotation Speed (RPM)	53					
3	Pressure (mm Hg)	700	500	300	700	500	300
	Voltage (kV)	40	38	27	39	30	25
	Capacitor Current (μ A)	220	700	750	89	145	82
	Ground Current (μ A)	240	650	720	115	160	105
	Rotation Speed (RPM)	110	81	42	90	75	47
4	Pressure (mm Hg)	700	500	300	700	500	300
	Voltage (kV)	42	36	25	46	36	25
	Capacitor Current (μ A)	130	133	650	307	450	350
	Ground Current (μ A)	160	170	600	340	370	350
	Rotation Speed (RPM)	128	118	60	138	105	62

When placed in a partial vacuum with a pressure less than 300 mmHg, no device showed signs of rotation, with one exception. When Device 2 was placed in the chamber and immediately pumped down to a pressure of 5.5×10^{-5} mmHg, something interesting

happened. The voltage on it was increased to 44 kilovolts, and through the viewing port a large arc was observed. At that same moment, the device was seen to move about a tenth of a rotation and stop. It appears likely that this was caused by material being ejected from the device, due to the arc. This material could be either copper atoms or moisture that had attached itself to the device when the vacuum chamber had been open to room air.

The data show an increase in the force produced by each device as the voltage applied to the device is increased. The voltages shown in Tables 3 through 5 are one or two kV below the pressure where arcing occurred. The voltage across a device without arcing decreased with pressure through 10^3 mmHg, followed by a sharp rise at 10^4 mmHg, to a voltage above that of near atmospheric pressure. This feature is well known in high voltage engineering. In virtually all cases, wiring configuration D allowed a greater voltage across the device and current through the device than configuration A.

The current through a device during runs where no rotation occurred showed a distinct feature; much greater current was measured (up to 4 times larger) during runs without motion than was measured during runs where the device rotated. During chamber testing, there were multiple runs where more current was measured to pass through the power supply into the device than out of it through the wire to ground. That is, some current was apparently making it to ground through the air, rather than from the wire to ground. However, in many cases the current taking this path through the air must have had the opposite "sign," as it decreased the total current (see Table 3 and note the total current is labeled the ground current there, due to how it is measured.)

Devices 3 and 4, when placed in a nitrogen environment, rotated with wiring configuration A, but not D. However, large currents flowed through the devices when in configuration D, in spite of the same or lower voltages across the devices. These results are shown in Table 4.

Table 4 Device Performance in Nitrogen

Device		Configuration A	Configuration D
3	Pressure (mm Hg)	700	700
	Voltage (V)	24	29
	Capacitor Current (μ A)	30	753
	Ground Current (μ A)	44	743
	Rotation Speed (RPM)	30	0
4	Pressure (mm Hg)	700	700
	Voltage (V)	33	25
	Capacitor Current (μ A)	77	750
	Ground Current (μ A)	100	740
	Rotation Speed (RPM)	90	90

While Device 4 was in an argon environment, it rotated on only one run, with wiring configuration B. Even though other wiring configurations achieved similar voltages and currents, no movement occurred in a configuration other than B. Data for the measurements which were made in the argon environment data were shown in Table 5.

Table 5 Device Performance in Argon

Device		Configuration A	Configuration B	Configuration D
4	Pressure (mm Hg)	700	760	700
	Voltage (V)	10	19	17
	Capacitor Current (μ A)	27	67	67
	Ground Current (μ A)	92	80	100
	Rotation Speed (RPM)	0	< 30	0

In the preliminary test chamber some unexpected results were noted. Device 1 when configured with wiring schematics B and C and Device 2 when wired in configuration B, were observed to turn backwards (towards the larger electrode) slowly (<30 RPM). While turning in the opposite direction of the other devices, voltage and current did not vary from that of other configurations. Device 2 C, however, turned in the same direction as all other devices. Device 2 with wiring configuration D did not perform as expected and showed no sign of rotation in spite of typical voltage and current measurements during the test.

An explanation for the change in the direction of motion for circuits C and D for the more symmetric Devices, 1 and 2, has been found. That explanation and supporting numerical computations will be given in detail in a separate publication². However, the basic idea is quite simple. The motion will be in the direction of the electrode that creates ions, regardless of the sign of their charge. Ions will be created on the electrode having the strongest electric field near its surface. It is the combination of the geometry of the body and the location of the ground which determines where there is the strongest electric field. For Devices 1 and 2 the geometry asymmetry is relatively weak, so the location of the ground are more important. For Devices 3 and 4 the wires from the screen provide a nearly discontinuous voltage which produces a strong electric field regardless of the location of the ground.

QUANTITATIVE ANALYSIS OF THE DATA

The force produced by the two ACTs mounted on the test fixture, computed from the friction overcome, is calculated by:

$$F = \frac{I\alpha}{r}$$

I is the moment of inertia of the entire rotational mechanism, *α* is the angular deceleration due to friction at a given rotational speed, and *r* is the moment arm from each ACT to the axis of rotation. For Device 4 spinning at 128 RPM in air at 700 Torr the force is:

$$F = \frac{.007666 \text{ kg m}^2 \times .65 \text{ rad/s}^2}{.178 \text{ m}} = .028 \text{ N}$$

We have developed a model of how the force is produced. That model assumes that Nitrogen ions undergo multiple collisions as they move from one electrode to the other under the influence of electrostatic forces². The resulting formula for the force produced is

$$F = 2d(10^{10} / \text{sec})mJ/e$$

In this formula, d is the distance the ions travel, $10^{10}/\text{sec}$ is the collision frequency of molecules in air at atmospheric pressure, J is the current flowing, and e is the charge on an ion. The sign of F is not meaningful. Since for Device 4 the gap is seven centimeters,

$$F = 0.14 \text{ meters}(10^{10} / \text{sec})4.7 * 10^{-26} \text{ Kg}1.6 * 10^{-4} \text{ Amps} / (1.6 * 10^{-19} \text{ Coulombs}) = 0.033 \text{ N}$$

It is gratifying that the formula, which assumes all of the current is used productively, produces a force (0.033 Newtons) which is slightly greater than that measured (0.028 Newtons). For all of the other tests reported here, the predicted force (without taking any loss mechanisms into account) was also greater than the measured force. Some were significantly greater. Using the understanding of the operation of this device, it is possible to make some observations about its efficiency. These observations show how to design devices that are more energy efficient.

The power used by this same device is equal to the voltage applied times the current flowing, which is

$$\text{Power consumed} = 42 * 10^3 \text{ Volts} * 1.6 * 10^{-4} \text{ Amps} = 6.72 \text{ Watts}$$

The power produced may be computed by taking the measured force times a velocity, which is

$$\text{Power produced} = 0.028 \text{ N} * 128 * 6.28 * 0.179 \text{ meters} / 60 \text{ sec} = 0.0668 \text{ Watts}$$

The ratio of power consumed to power produced is about 100:1. However, this is not an intrinsic limitation of ACTs. If it had been allowed to rotate twice as fast (using different bearings), then approximately twice as much power would have been produced.

To put this 100:1 ratio in perspective, we compute the velocities of the ACT in operation and of an ion at each collision. The ACTs are moving at a speed

$$\text{Speed of ACT} = 128 * 6.28 * 0.178 \text{ meters} / 60 \text{ sec} = 2.38 \text{ meters/second}$$

The speed of an ion at a typical collision is given by its acceleration times the time between collisions,

$$\begin{aligned}\text{Speed of Ion} &= 10^{-10} \text{ sec} * 1.6 \cdot 10^{-19} \text{ Coul.} * 42 * 10^4 \text{ V} / (0.07 \text{ meters} * 4.7 \cdot 10 \text{ Kg}) \\ &= 204.26 \text{ meters/second}\end{aligned}$$

We notice that the ratio of these speeds is almost exactly 100:1. It is no coincidence that these two ratios are almost identical. The efficiency is reduced because more energy is lost to collisions between the ions and air molecules than is used due to the rotation of the device.

This insight suggests how to make the ACT more efficient. One may run it with a lower ratio of voltage to distance, or at a lower average electric field between the plates. This could be accomplished by decreasing the voltage or by increasing the gap between the electrodes. However, as the average electric field between the plates is lowered, the large electric field in the vicinity of one plate must be maintained. That is necessary to create enough ions so that the required current flows.

CONCLUSIONS

Several types of Asymmetrical Capacitor Thrusters (ACTs) have been designed and tested. A series of improved designs has led to an understanding of how to design a device for maximum thrust and efficiency. A series of tests in a vacuum chamber documented their performance in air, argon and nitrogen at atmospheric pressure and at reduced pressures. However, none of the designs tested produced a force below 300 Torr. That pressure is not likely to represent an intrinsic limitation; it just was the limitation for the devices that were tested which were all designed for atmospheric pressure. The understanding gained suggests how to design ACTs to operate at reduced pressures. Both the understanding and the test results obtained here suggest that these devices cannot operate in a complete vacuum. A theoretical formula was introduced which computes the force due to an ACT. This formula was based on electrostatic forces interacting with a current of ions drifting from one electrode of the capacitor to the other, and on those ions giving momentum to the ambient atmosphere through multiple collisions. This theory (semi) quantitatively predicted the forces that were measured. It also showed how to improve their energy efficiencies. It appears that now the main features of the functioning of ACTs are well understood, as are many of the engineering issues of their efficient design for different purposes.

References

1. Brown, T.T., GB Patent 300,311, "A Method of and an Apparatus or Machine for Producing Force or Motion", 1928.
2. Canning, Francis X., Melcher, Cory, and Winet, Edwin, Asymmetrical Capacitors for Propulsion, submitted to AIAA Journal of Propulsion and Power.
3. Campbell, J.W., US Patent 6,317,310, "Apparatus and Method for Generating Thrust Using a Two Dimensional, Asymmetrical Capacitor Module", 2001.
4. Campbell, J.W., US Patent 6,411,493, "Apparatus and Method for Generating Thrust Using a Two Dimensional, Asymmetrical Capacitor Module", 2002.